INL/EXT-21-61961

Modeling and Analysis Support for High Temperature Single Heat Pipe Experiment: Current Status and Plan

March 2021

JunSoo Yoo, Sunming Qin, Minseop Song, Jeremy L. Hartvigsen, Zackary D. Sellers, Terry J. Morton, Piyush Sabharwall, Joshua Hansel
Idaho National Laboratory

Lander Ibarra, Bo Feng
Argonne National Laboratory

Christian M. Petrie
Oak Ridge National Laboratory

MRP Microreactor Program

NEAMS NUCLEAR ENERGY ADVANCED MODELING & SIMULATION PROGRAM

INL Idaho National Laboratory

INL is a U.S. Department of Energy National Laboratory
operated by Batelle Energy Alliance, LLC

INL/EXT-21-XXXXX

Modeling and Analysis Support for High Temperature Single Heat Pipe Experiment: Current Status and Plan

JunSoo Yoo, Sunming Qin, Minseop Song, Jeremy L. Hartvigsen, Zackary D. Sellers, Terry J. Morton, Piyush Sabharwall, Joshua Hansel
Idaho National Laboratory
Lander Ibarra, Bo Feng
Argonne National Laboratory
Christian M. Petrie
Oak Ridge National Laboratory

March 2021

Idaho National Laboratory
Originating Organization NS&T
Idaho Falls, Idaho 83415

http://www.inl.gov

Prepared for the
U.S. Department of Energy
Office of NE
Under DOE Idaho Operations Office
Contract DE-AC07-05ID14517

Page intentionally left blank

SUMMARY

This report summarizes the modeling and simulation activities under DOE microreactor program to support ongoing single heat pipe experiments with 7-hole core block at the SPHERE facility. The primary objective of these activities is to obtain preliminary insights into the current single heat pipe-cooled experimental facility, and based on that, support and guide the experimental efforts and test plans with the aim of producing high-quality experimental data.

Considering the current major interests of the single heat pipe experiment, i.e., (i) the startup behavior of liquid-metal heat pipe and (ii) the thermal stress of structural materials under high temperature operating conditions, the modeling and simulation efforts are being made in two respects:

(1) Development of a simplified conduction-based heat pipe analysis method for analyzing the liquid metal (sodium) heat pipe startup from a frozen state

(2) A coupled thermal-structural modeling and analysis for SPHERE experiment (with 7-hole core block) and code-to-code benchmark

As of February 2021, the theoretical development of the conduction-based heat pipe startup analysis model and the preliminary model performance tests using commercial CFD software have been completed. Also, the FEM-based coupled thermal-stress analysis model for the ongoing single heat pipe experiment has been created using the two commercial software packages (ABAQUS and STAR-CCM+), and the code-to-code benchmark study has been performed. The analysis results have led us to identify the limitations of the current models and future tasks for model improvement and validation.

Efforts will continue to use and further develop the modeling and analysis capabilities that have been built so far, to support ongoing single heat pipe experimental activities at the SPHERE facility such as measurement planning, data analysis, and potential design improvement study. In addition, continuing collaboration with the NEAMS program is considered important so that the experimental data from SPHERE can satisfy the validation needs of Sockeye, a system-level heat pipe modeling software being developed with the support of DOE.

Page intentionally left blank

ACKNOWLEDGEMENTS

This research was supported by the U.S. Department of Energy Office of Nuclear Energy Microreactor Research and Development Program under U.S. Department of Energy Contract No. DE-AC07- 05ID14517. This research also made use of the resources of the High-Performance Computing Center at Idaho National Laboratory, which is supported by the U.S. Department of Energy Office of Nuclear Energy and the Nuclear Science User Facilities, and authored by Battelle Energy Alliance, LLC, under Contract No. DE-AC07-05ID14517. This work acknowledges support from Department of Energy Nuclear Energy Advanced Modeling and Simulation program.

Page intentionally left blank

CONTENTS

FIGURES

TABLES

Page intentionally left blank

NOMENCLATURE

A	Area [m^2]
c_p	Specific heat [J/kg-K]
D	Diffusion coefficient [m^2/s]
h	Enthalpy [J/kg]
h_{lv}	Latent heat of vaporization [J/kg]
H	Latent heat of melting or freezing [J/kg]
k	Thermal conductivity [W/m-K] or Boltzmann constant [J/K]
$k_{eff,v}$	Effective conductivity of vapor [W/m-K]
L_a	Length of adiabatic section [m]
L_c	Length of condenser [m]
L_e	Length of evaporator [m]
L_t	Total length of heat pipe [m]
$\dot{m}$	Mass flow rate [kg/s]
M_g	Molar mass [kg/mol]
N_A	Avogadro number
P	Pressure [Pa]
$\dot{q}$	Heat transfer rate due to phase change per unit length [W/m]
Q	Heat flow rate [W]
R	Radius [m]
R_g	Gas constant [J/kg-K]
T	Temperature [K]

SUBSCRIPTS

c	Vapor core
i	Phase state (i.e., solid, liquid, vapor)
in	Input
init	Initial condition
l	liquid
pc	phase change
m	melting
s	Solid
v	vapor
w	wall
ws	wick structure

GREEKS

γ	Specific heat ratio [-]
ρ	Density [kg/m3]
ε	porosity

Page intentionally left blank

Modeling and Analysis Support for High Temperature Single Heat Pipe Experiment: Current Status and Plan

1. INTRODUCTION

Microreactor systems produce a stable, continuous supply of abundant energy in a relatively small footprint. For microreactors specific deployment opportunities may include provision of heat and electrical power to remote commercial and industrial applications, remote civilian municipalities, or remote or islanded military installations. Various types of microreactor designs are under consideration, in this report the emphasis is on heat pipe cooled reactor designs. This report provides an overview of the current modeling and analysis tools that are being used to support experimental needs of the high temperature single heat pipe experiment for single primary heat extraction and removal emulator (SPHERE) facility, along with Sockeye (based on multiphysics object-oriented simulation environment framework) verification and validation (V&V) approach. The V&V methodology will be used to demonstrate the adequacy of the code for evaluation of safety performance (performance limits) and characterization of safety margins for heat pipes, which will further assist with design, development, and demonstration of heat pipe cooled microreactors.

2. EXPERIMENTAL CAPABILITITES

The SPHERE facility is equipped with a test chamber that allows for either vacuum (10^{-4} torr) or inert gas operation. The test chamber is an 8-ft long, 6-inch diameter quartz tube with flanges for gas flow connections and instrumentation feedthrough ports.

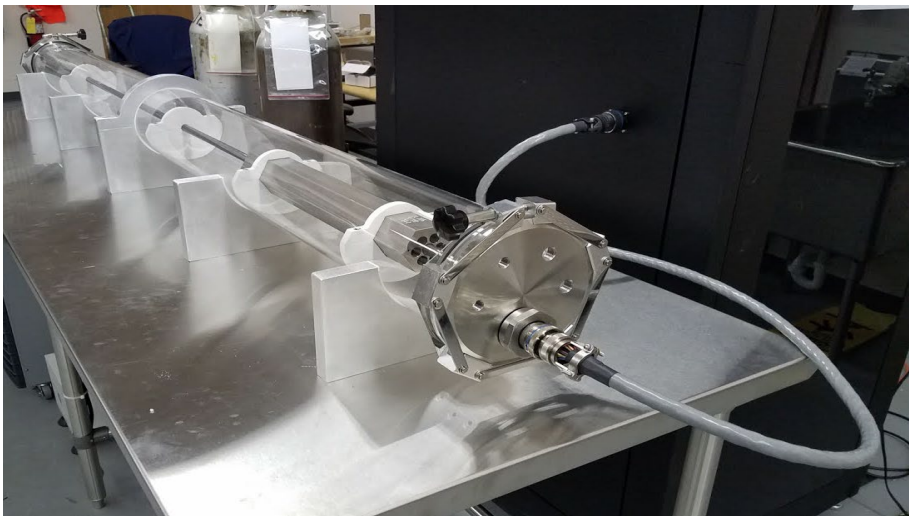

Figure 1. SPHERE test bed and seven-hole test article.

The electrical capabilities of the test bed allow for up to 20 kW of electrical power to be supplied to the heaters. The maximum operating temperature for the test article is 750 °C. For the initial test, heat was rejected through passive radiation, but for future operations a water-cooled gas gap calorimeter will be installed to allow for calorimetric measurements to be obtained.

The initial test article was equipped with a thermowell that allowed for a type K multipoint thermocouple with ten points to be used to get internal temperature measurements along the axis of the heat pipe. External thermocouples, also type K, were spot welded to the outside of the heat pipe as well as

on the outside of the hex block using 5 Mil stainless steel straps to get a better temperature distribution of both the heat pipe, and the hex block.

For future experimental tests, strain gauges will be installed to get an accurate measurement of stress on both the heat pipe and the hex block. All the instrumentation is interfaced to a LabVIEW virtual instrument for data acquisition and instrument control.

The heat pipe is heated utilizing cartridge heaters. The cartridge heaters have a maximum heat-flux value of 3.8 W/cm^2. This value was selected to mimic the expected microreactor core power densities. Each heater is also interfaced to a LabVIEW virtual instrument. The power supplied to each heater is continuously monitored using precision power meters designed for measurements of SCR-controlled loads. This is done utilizing Watlow Din-A-Mites silicon-controlled-rectifier (SCR)-based power controllers.

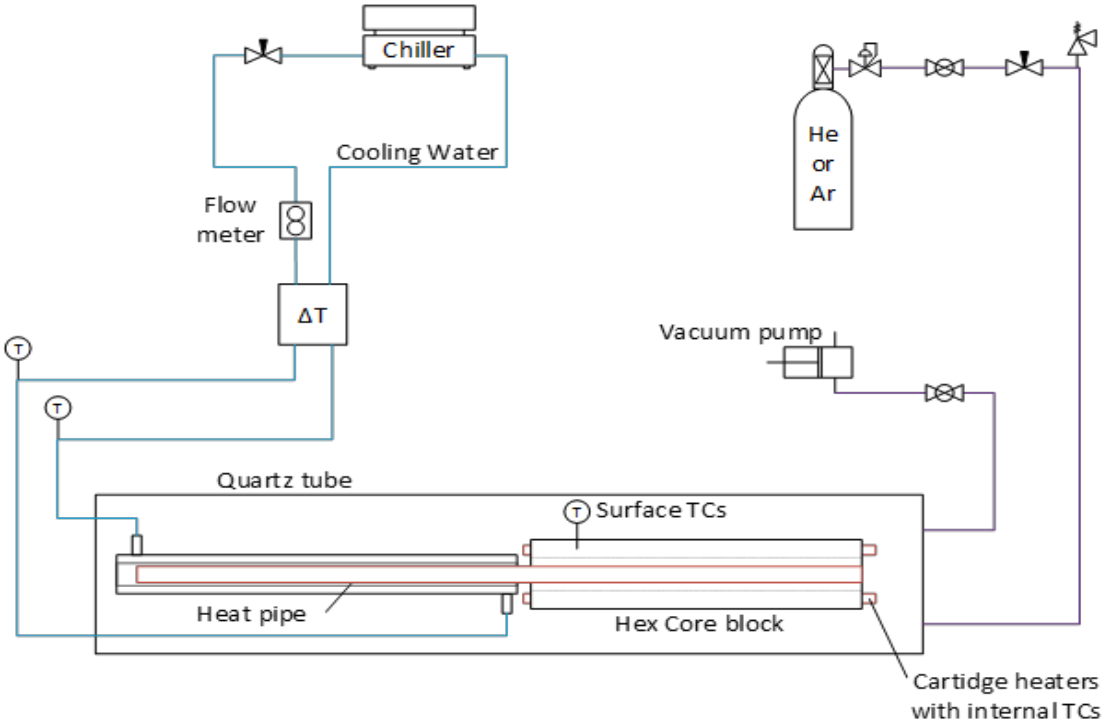

Figure 2. Piping and instrumentation diagram for the SPHERE facility.

3. MODELING AND ANALYSIS TO SUPPORT EXPERIMENTS

3.1 Modeling Needs and Current Status

Modeling and simulation can serve to provide relevant insights throughout the entire experimental procedure, from design, experimental data analysis (for the physics not directly captured by experiments) to measurement planning. In this regard, the DOE microreactor program supports the modeling and simulation activities for the ongoing single heat pipe experiments at SPHERE facility with the aim of producing high fidelity experimental data. Given that the MOOSE-based heat pipe modeling software, Sockeye, is still in development, the current modeling and simulation efforts focus on leveraging commercial software packages.

Among the major concerns of the single heat pipe experiment are the startup behavior of the sodium heat pipe from a frozen state, associated heat pipe performance limits, and the resulting behavior of the heat pipe-cooled system. Another important aspect that should be well understood through this experiment efforts is the potential concern of thermal stress across the structural materials in the high temperature operating conditions of microreactors, especially near the places where large temperature

gradients exist. In order to effectively achieve these goals and support the production of high-quality experimental data, modeling and analysis efforts are currently underway in two aspects:

1. Development of a simplified conduction-based heat pipe analysis method for analyzing the liquid metal (sodium) heat pipe startup from a frozen state.
2. A coupled thermal-structural modeling and analysis for SPHERE experiment (with 7-hole core block) and code-to-code benchmark.

The primary objective of these efforts is to gain preliminary insight into the current single heat pipe experiment, and based on that, guide/support the ongoing experimental activities and test plans. The following subsections summarize the current status of each activity [i.e., (1) and (2)], including the models/methods description, preliminary analysis, and validation results.

3.1.1 Theoretical Development

In the present approach, we attempt to simulate the entire startup process of the liquid-metal heat pipes, including the melting of working fluid and growth of continuum vapor flow along a heat pipe, based solely on heat conduction equations. The key to this model development is to derive the effective thermal conductivity of gaseous phase of working fluid (i.e., vapor) by employing appropriate simplifying physical assumptions. For example, the viscous dissipation and axial conduction within the vapor core of a heat pipe, gravitational effect, and liquid flow through porous wick structure were neglected in the present modeling approach. Since the present modeling approach relies purely on heat conduction equation, it is easy to be implemented by user-defined functions in any commercial CFD software packages.

The derivation of effective thermal conductivity of gaseous phase working fluid within a vapor core of liquid-metal heat pipes and modeling assumptions employed are summarized below.

Figure 3 shows the simplified heat and mass transfer processes occurring around an arbitrary vapor cell within a heat pipe and based on this, the mass balance and energy balance equations can be formulated as shown in Eqs. (1) and (2), respectively.

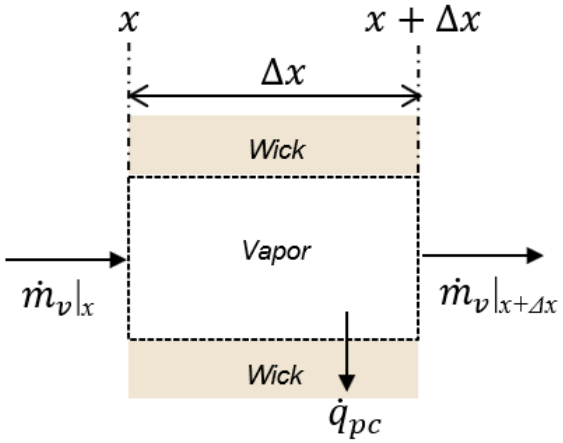

Figure 3. Simplified heat and mass transfer processes around an arbitrary vapor cell in a heat pipe.

$$\dot{m}_v|_x - \dot{m}_v|_{x+\Delta x} - \frac{\dot{q}_{pc}\Delta x}{h_{lv}} = 0 \tag{1}$$

$$d(Q_v) = \Delta x \frac{dU_v}{dt} = \dot{m}_v h_v|_x - \dot{m}_v h_v|_{x+\Delta x} - \dot{q}_{pc}\Delta x \tag{2}$$

(where $\dot{q}_{pc}$ is the heat transfer rate due to the phase change (i.e., evaporation or condensation) per unit length of a heat pipe [W/m], $\dot{m}_v|_x$ is the mass flow rate of vapor at the axial location x [kg/s], h_{lv} is the latent heat of vaporization [J/kg], Q_v is the heat flow rate of vapor [W], and U_v is the internal energy of vapor per unit length [W/m].)

The Eqs (1) and (2) can be re-expressed as:

$$d(\dot{m}_v) = \frac{\dot{q}_{pc}\Delta x}{h_{lv}} \tag{3}$$

$$d(Q_v) = \Delta x \frac{dU_v}{dt} = d(\dot{m}_v h_v) - \dot{q}_{pc}\Delta x \tag{4}$$

Using the relation of Eq. (3), the Eq (4) can be re-written as:

$$d(Q_v) = \Delta x \frac{dU_v}{dt} = d(\dot{m}_v h_v) - h_{lv} d(\dot{m}_v) \tag{5}$$

If there is no phase change such as in the adiabatic section of a heat pipe, the second term of Eq. (5) can be neglected because the change of vapor mass flow rate is equal to zero [i.e., $d(\dot{m}_v) = 0$]. For the evaporator and condenser sections of a heat pipe where phase change occurs, if the latent heat of vaporization (h_{lv}) is assumed to be constant, the Eq. (5) can be written as:

$$\begin{aligned} d(Q_v) = \Delta x \frac{dU_v}{dt} &= d(\dot{m}_v h_v) - d(\dot{m}_v h_{lv}) \\ &= d(\dot{m}_v h_l) \end{aligned} \tag{6}$$

Then, the heat transfer rate of vapor along a heat pipe can be expressed, depending on whether phase change occurs or not, as follows:

$$Q_v = \dot{m}_v h_l \quad \text{(for evaporator and condenser sections)} \tag{7}$$

$$Q_v = \dot{m}_v h_v \quad \text{(for adiabatic section)} \tag{8}$$

According to Fick's law,

$$\dot{m}_v^{"} = \frac{\dot{m}_v}{\pi R_v^2} = -D \frac{d\rho}{dx} \tag{9}$$

(where $\dot{m}_v^{"}$ is vapor mass flux, $\dot{m}_v$ is vapor mass flow rate [kg/s], D is diffusion coefficient [m^2/s], R_v is the radius of vapor core [m], and ρ is vapor density [kg/m^3].)

Using the ideal gas law ($P=\rho R_g T$), the right term of Eq. (9) can be re-written as follows:

$$-D \frac{d\rho}{dx} = -\frac{D}{R_g T} \frac{dP}{dx} = -\frac{M_g D}{N_A k T} \frac{dP}{dx} \tag{10}$$

(where R_g is gas constant [J/kg-K], M_g is molar mass [kg/mol], N_A is Avogadro number, k is Boltzmann constant [J/K], T is temperature [K], and P is pressure [Pa].)

From Eqs. (9) and (10), the vapor mass flow rate ($\dot{m}_v$) can be expressed as:

$$\dot{m}_v = -\pi R_v^2 \frac{M_g D}{N_A k T} \frac{dP}{dx} \tag{11}$$

Then, by inserting the Eq. (11) into Eqs. (7) and (8) the heat transfer rate of vapor (Q_v) can be written as follows:

$$Q_v = \dot{m}_v h_l = -D \frac{\pi R_v^2 h_l M_g}{N_A k T} \frac{dP}{dx} \text{ (for evaporator and condenser)} \tag{12}$$

$$Q_v = \dot{m}_v h_v = -D \frac{\pi R_v^2 h_v M_g}{N_A k T} \frac{dP}{dx} \text{ (for adiabatic section)} \tag{13}$$

Assuming the saturated condition of vapor, which has been widely used and proven to be reasonable in heat pipe modeling [1-4], the Clausius-Clapeyron relation can be employed:

$$\frac{dP}{dT} = \frac{\rho_v h_{lv}}{T} \tag{14}$$

The saturated vapor assumption also allows us to apply the chain rule on the pressure gradient terms in Eqs. (12) and (13) as shown below, due to the one-to-one relation between the pressure and temperature:

$$\frac{dP}{dx} = \frac{dP}{dT}\frac{dT}{dx} \tag{15}$$

Incorporating the relations of Eqs. (14) and (15) into Eqs. (12) and (13) results in

$$Q_v = -D\frac{\pi R_v^2 h_l M_g}{N_A kT}\frac{dP}{dT}\frac{dT}{dx} = -D\frac{\pi \rho_v R_v^2 h_l h_{lv} M_g}{N_A kT^2}\frac{dT}{dx} \text{ (for evaporator and condenser)} \tag{16}$$

$$Q_v = -D\frac{\pi R_v^2 h_v M_g}{N_A kT}\frac{dP}{dT}\frac{dT}{dx} = -D\frac{\pi \rho_v R_v^2 h_v h_{lv} M_g}{N_A kT^2}\frac{dT}{dx} \text{ (for adiabatic section)} \tag{17}$$

Subsequently, by applying the ideal gas law ($P=\rho_v R_g T$) to the Eqs. (16) and (17) the following equations are obtained:

$$Q_v = -D\frac{\pi R_v^2 h_l h_{lv} M_g P}{R_g N_A kT^3}\frac{dT}{dx} \text{ (for evaporator and condenser)} \tag{18}$$

$$Q_v = -D\frac{\pi R_v^2 h_v h_{lv} M_g P}{R_g N_A kT^3}\frac{dT}{dx} \text{ (for adiabatic section)} \tag{19}$$

(where R_g is gas constant [J/kg-K].)

It is noted that Eqs. (18) & (19) have analogous forms with Fourier's law, so similar to the approach of Ma et al. [4], we can obtain the effective thermal conductivity of vapor within the heat pipe based on the following equations:

$$Q_v = -D\frac{\pi R_v^2 h_l h_{lv} M_g P}{R_g N_A kT^3}\frac{dT}{dx} = -k_{eff,v}A_v\frac{dT}{dx} \text{ (for evaporator and condenser)} \tag{20}$$

$$Q_v = -D\frac{\pi R_v^2 h_v h_{lv} M_g P}{R_g N_A kT^3}\frac{dT}{dx} = -k_{eff,v}A_v\frac{dT}{dx} \text{ (for adiabatic section)} \tag{21}$$

[where $k_{eff,v}$ is the effective thermal conductivity of vapor and A_v is the cross-sectional area of vapor core within a heat pipe ($=\pi R_v^2$).]

From Eqs. (20) and (21), the effective thermal conductivity of vapor ($k_{eff,v}$) is obtained as follows:

$$k_{eff,v} = -D\frac{h_l h_{lv} M_g}{R_g N_A kT^3}P \text{ (for evaporator and condenser)} \tag{22}$$

$$k_{eff,v} = -D\frac{h_v h_{lv} M_g}{R_g N_A kT^3}P \text{ (for adiabatic section)} \tag{23}$$

(where P is the saturated vapor pressure [Pa] at a given vapor temperature T [K].)

For evaluating the diffusion coefficient D in Eqs (22) and (23), the Dusty-Gas-Model [5] was employed in the present work.

3.1.2 Heat Pipe Startup Analysis Model Description

The commercial code STAR-CCM+ version 15.06 has been used to verify the performance of the proposed conduction-based heat pipe startup analysis model. In the present work, only heat conduction equations are solved for the different regions of a heat pipe (i.e., wall, wick, and vapor core), as a conjugate problem, to simulate the entire process of heat pipe startup from a frozen state. The effective thermal conductivity of vapor, derived in Section 3.1.1, was implemented in STAR-CCM+ as user-defined function, to model the growth of continuum vapor region along the heat pipe (vapor region) during startup. To reduce the computational cost, the transient conduction analysis was carried out using 2D mesh axisymmetric model.

For the numerical solvers, to overcome the challenge of applying a fully coupled method for the entire region of heat pipe (i.e., wall, wick, and vapor regions), due to the large difference of physical time scales between vapor and wall/wick regions, the hybrid numerical approach was employed, meaning that the transient conduction solver was used for the analysis of wall/wick regions while the vapor region was solved with steady-state conduction solver. In this approach, one of the boundary conditions for the steady-state solver (i.e., wick-vapor interface) is updated at each time step by the transient simulation

result of the wick region, as shown in Figure 4. The steady-state solution at the wick-vapor interface is also used as a boundary condition for the transient simulation for the wall/wick regions at the subsequent time step. The quasi steady-state assumption of the vapor region can be justified by the fact that the vapor dynamics has much smaller time scale than the wall or wick conduction. The similar approach was taken by Zuo and Faghri [6] with the justification of this hybrid modeling approach based on the dimensional analysis. This method helped reduce the computation time and improve the convergence compared to the fully coupled transient method in our tests. It should be noted, however, the quasi steady assumption of vapor may introduce substantial errors if the magnitude of heating or cooling source terms become very large [6], thus caution is required. For the present study, this hybrid approach was realized in STAR-CCM+ using the multiple time scale function.

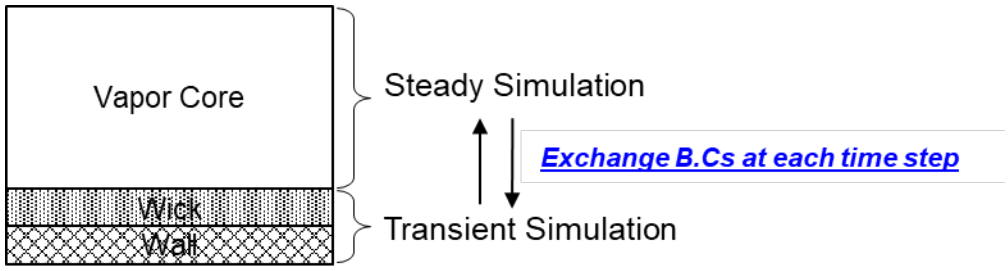

Figure 4. Hybrid numerical method applied to the present heat pipe startup analysis study.

The focus of present work is to simulate the entire startup process of a 'sodium' heat pipe, considering the ongoing heat pipe experiment in the SPHERE facility.

The thermal properties of the component materials of sodium heat pipe, used in the preliminary model performance tests (Section 3.2.3), are summarized in Table 1. In the vapor core region of a sodium heat pipe, the temperature-dependent density (ρ) and specific heat (c_p) of the gaseous phase sodium was considered, but the thermal conductivity of sodium vapor was considered as described in Eqs. (22) and (23) instead of the actual thermal conductivity for the sodium vapor.

For the thermal properties of porous wick, the effective thermal properties were obtained based on the wick porosity (ε) measured from experiments, while the effect of liquid flow through the wick structure was neglected. In order to properly analyze the heat pipe startup from a frozen state, the phase change of the frozen working fluid within a porous wick must be considered.

Table 1. Thermal Properties of Materials for the Analysis of Sodium Heat Pipe Startup.

Heat Pipe Regions	Thermal Properties and Relevant Modeling Assumptions	Reference
Wall	Temperature-dependent properties (ρ, c_p, k) of SS-304.	[7]
Wick	• Temperature-dependent properties of sodium (ρ, c_p, k) in the liquid and solid states. • Effective thermal properties (ρ_{eff}, $c_{p,eff}$, k_{eff}) are computed based on the wick porosity (ε) of experiment [Eqs. (26)-(28)]. • Sodium melting during the startup phase is modeled using equivalent heat capacity method.	[1, 8, 9]
Vapor Core	• Temperature-dependent density (ρ) and specific heat (c_p) of gaseous phase sodium. • k_{eff} of sodium vapor derived in Section 3.2.1.	[3, 10]

The phase change of working fluid (i.e., melting of sodium) within the porous wick structure was modeled using the equivalent heat capacity method [9].

$$c_{p,Na}(T) = \begin{cases} c_{p,s} & if\ (T < T_m - \Delta T) \\ \frac{c_{p,s}+c_{p,l}}{2} + \frac{H}{2\Delta T} & if\ (T_m - \Delta T \le T \le T_m + \Delta T) \\ c_{p,l} & if\ (T > T_m + \Delta T) \end{cases} \quad (24)$$

$$k_{Na}(T) = \begin{cases} k_s & if\ (T < T_m - \Delta T) \\ k_s + (k_l - k_s)\frac{(T - T_m + \Delta T)}{2\Delta T} & if\ (T_m - \Delta T \le T \le T_m + \Delta T) \\ k_l & if\ (T > T_m + \Delta T) \end{cases} \quad (25)$$

In Eqs. (24) and (25), ΔT=0.1 K was employed in the present works. Then, the effective density (ρ_{eff}) and specific heat ($c_{p,eff}$) within the heat pipe wick structure was computed as follows:

$$\rho_{i,eff} = \varepsilon\rho_i + (1-\varepsilon)\rho_{ws} \quad (26)$$

$$c_{i,eff} = \varepsilon c_i + (1-\varepsilon)c_{p,ws} \quad (27)$$

(where the subscript i refers to the phase state, i.e., 's' and 'l' denotes the solid and liquid phases of working fluid, respectively; the subscript 'ws' denotes the wick structure; ε denotes the porosity of the heat pipe wick.)

Assuming the homogenous and isotropic structure of a wick, the effective thermal conductivity within the heat pipe wick can be calculated using the following equation proposed by Chi [10]:

$$k_{eff,ws} = \frac{k_l[(k_l+k_s)-(1-\varepsilon)(k_l-k_s)]}{[(k_l+k_s)+(1-\varepsilon)(k_l-k_s)]} \quad (28)$$

It is very important to understand the heat pipe performance limit (or heat transfer limit) when analyzing the thermal behavior of heat pipe, including the startup process. In particular, it is well known that the sonic limitation is very significant during the startup phase of liquid-metal heat pipes [10]. The sonic limitation is usually dominant when heat pipes are operating at low temperatures with low vapor pressures (or low vapor densities) and high vapor velocities. At this limit, the maximum axial heat transport rate is limited due to the choked flow of vapor, and a certain degree of axial temperature drop occurs along the evaporator. The upper limit of axial heat transport rate due to sonic limit can be expressed using the Levy's equation [3, 10] as follow:

$$Q_{sonic}(T) = \frac{\rho_{v,0}A_c h_{lv}\sqrt{\gamma R_g T_{v,0}}}{\sqrt{2(\gamma+1)}} \quad (29)$$

In the present heat pipe startup analysis employing solely heat conduction equations, the effect of sonic limit can be considered using the following equations:

$$\oint k_{eff,v}\nabla T_{v,axial}\,dA \le Q_{sonic}(T) \quad (30)$$

$$k_{eff,v}(T) \le \frac{Q_{sonic}(T)}{A_c|\nabla T_{v,axial}|} \quad (31)$$

(where $\nabla T_{v,axial}$ is the vapor temperature gradient along the axial direction of a heat pipe and A_c is the cross-sectional area of the vapor core.)

Eventually, the Eq. (31) was implemented in STAR-CCM+ as user-defined function to model the effect of sonic limit that may occur during the frozen startup process. Figure 5 shows an example of the effect of sonic limit predicted by the present modeling approach during the sodium heat pipe startup process. This shows that the axial heat transport rate evaluated at the evaporator exit ('Q_evap,exit' in Figure 5) follows the sonic limit after about 500 sec, which implies that the axial heat transport rate is limited by the constraint employed, i.e., sonic limit.

The initial and boundary conditions that have been commonly applied for the present (conduction-based) heat pipe startup analysis is summarized in Table 2. The heat pipe temperature was initially assumed to be uniform across the entire heat pipe region. Also, the uniform heat flux was assumed on the outer surface of the heat pipe wall from the heater activated within the evaporator section. At the outer wall of condenser section, the radiative heat transfer (or loss) was assumed based on the emissivity value measured from experiments [11, 12].

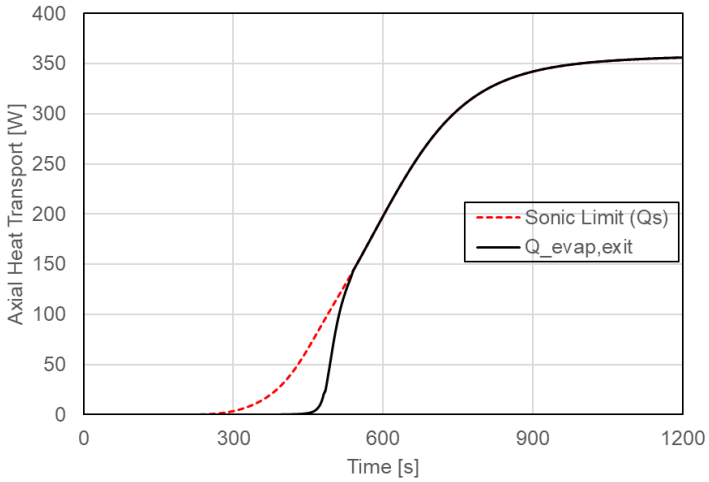

Figure 5. Axial heat transport capacity through the evaporator exit, precited by the present model, during the sodium heat pipe startup process.

Table 2. Initial and Boundary Conditions for the Present Analysis of Sodium Heat Pipe Startup.

Heat Pipe Regions	Initial and Boundary Conditions
Wall	$T_{init,w}$=uniform (given from experiment) For $r=R_0$ (heat pipe outer wall surface): $k_w \frac{\partial T}{\partial r} = q_e^{"}$ $(0 \le z \le L_e)$ $\frac{\partial T}{\partial r} = 0$ $[L_e \le z \le (L_e + L_a)]$ $-k_w \frac{\partial T}{\partial r} = \sigma\epsilon(T_w^4 - T_\infty^4)$ $[(L_e + L_a) \le z \le L_t)$ For evaporator and condenser end caps: $\frac{\partial T}{\partial x} = 0$ at $x=0$ and $x=L_t$
Wick	$T_{init,wick}$=$T_{init,w}$=uniform For evaporator and condenser end caps: $\frac{\partial T}{\partial x} = 0$ at $x=0$ and $x=L_t$
Vapor Core	$T_{init,wick}$=$T_{init,v}$=uniform For evaporator and condenser end caps: $\frac{\partial T}{\partial x} = 0$ at $x=0$ and $x=L_t$

3.1.3 Preliminary Model Performance Test and Validation

Based on the modeling approach described in Sections 3.2.1 and 3.2.2, the sodium heat pipe experiments performed by three different authors, (i) Faghri et al. [1, 11], (ii) Buchko [13], and (iii) Ponnappan [14] were modeled and simulated in the present work. Then, the model prediction results using STAR-CCM+ were compared with the experimental data (i.e., temperature measured from heat pipe outer wall during startup). The mesh independence study as well as the sensitivity study on the time step size (Δt) were performed to ensure the converged numerical solution with reasonable accuracy, but the details of them are not presented in this report. Considering the accuracy of numerical solution and computational cost, the time step size of 0.02 sec was used for all the sodium heat pipe startup simulations presented below.

The numerical simulation was first performed for the sodium heat pipe experiments of Faghri et al. [12] and Buchko [13]. The sodium heat pipe studied by Faghri et al. [12] and Buchko [13] had multiple heaters within the evaporation section, as shown in Figure 6. The heat pipe contained a vapor core with a radius of 10.75 mm, a wrapped screen wick of 0.456 mm thick, and stainless steel (SS-304) wall of 2.15 mm thick. The portion of each individual heater (evaporator) is denoted by '(1)' in Figure 6. The sodium heat pipe experiments, numerically simulated in the present work, were tested in a vacuum chamber with a fluid charge of 30g of sodium [1, 14]. It is important to note that in the present simulations, an estimated additional heat capacity of 3.75×10^6 [J/m^3-K] was considered in the evaporator and adiabatic sections to account for the additional heat capacities caused by the electrical resistance heaters and radiation shields, as proposed by Cao and Faghri [1].

For more details on the experimental setup, heat pipe dimensions, and test boundary conditions (heat inputs and outputs), the readers are advised to refer to Buchko [13] and Faghri et al. [12].

Figure 7 compares the outer wall temperatures measured over time, by Faghri et al. (left) and Buchko (right), and the numerical simulations during the sodium heat pipe frozen startup. The test cases presented in Figure 7 correspond to the 'case 11a' of Faghri et al. experiment [12] and 'case19a' of Buchko experiment [13], respectively. In both experiments, only the evaporator 1 (marked as solid red rectangle in Figure 6), which is closest to the evaporator end cap, was activated during the experiments. Figure 7 shows that the numerical simulations predict the evolution of the hot zone front measured by the two experiments generally well.

Another sodium heat pipe experiment, studied by Ponnappan [14], was also modeled and simulated in the present work. The sodium heat pipe studied by Ponnappan was a 2 m long double-wall artery gas-loaded heat pipe, in which there was a vapor core with a radius of 6.35 mm, an outer wall with a radius of 11.1mm and a stainless steel of 1.65mm thick. The lengths of each heat pipe section were, as shown in Figure 8, 375 mm (evaporator), 745 mm (adiabatic section), and 910 mm (condenser).

The numerical simulation, using the present conduction-based model, was performed for the experimental case with the heat input Q_{in}=289W from the evaporator. Figure 9 shows that the simulation predicts the outer wall temperature measured by the experiment reasonably well.

The comparisons, between the experimental data generated from the different designs of sodium heat pipe with different heat inputs and model predictions, show that the present conduction-based model predicts the startup behavior of the sodium heat pipes, specifically the evolution of the hot zone front during startup, reasonably well.

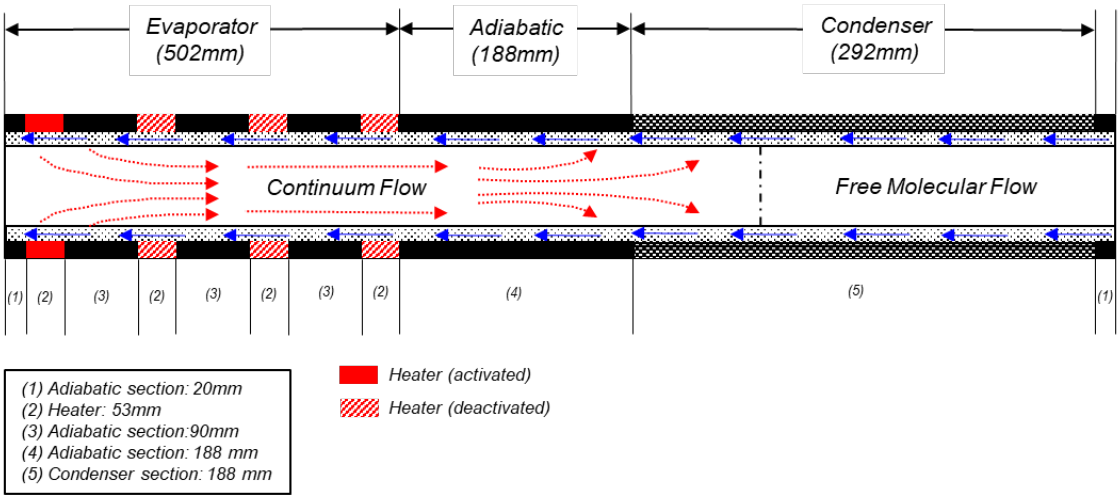

Figure 6. Schematic of sodium heat pipe experiment of Faghri et al.[12]

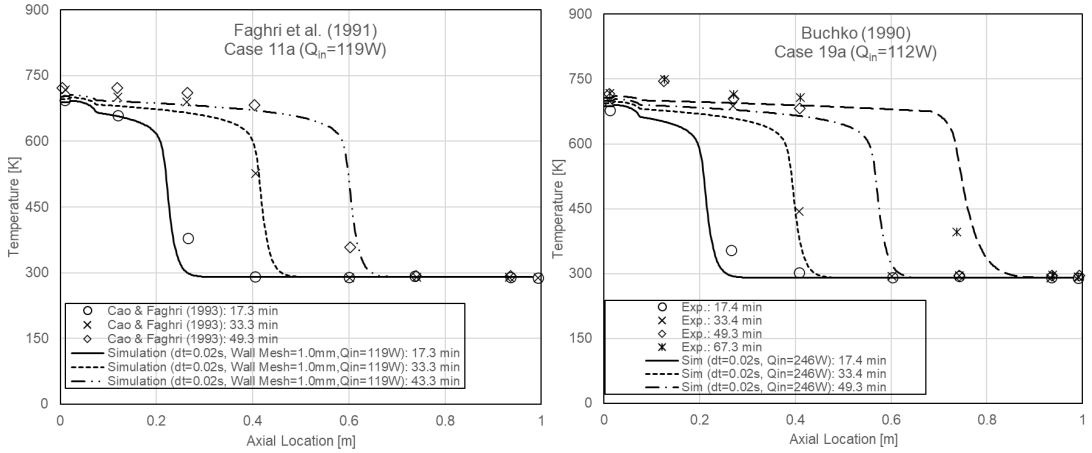

Figure 7. Predicted outer wall temperature compared against experiment of Cao and Faghri (left) [1] and Buchko (right). [13]

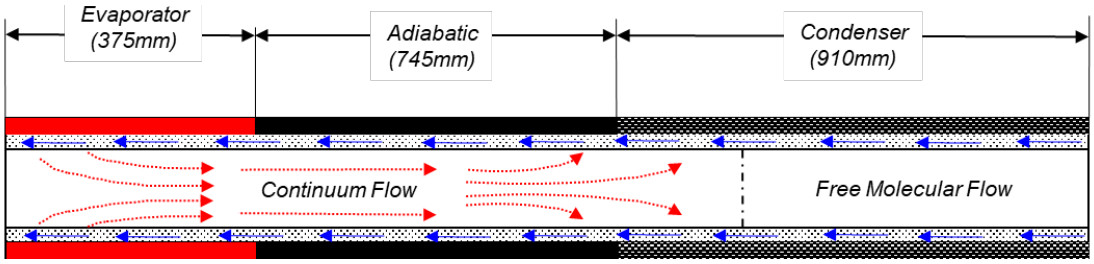

Figure 8. Schematic of sodium heat pipe experiment Ponnappan. [14]

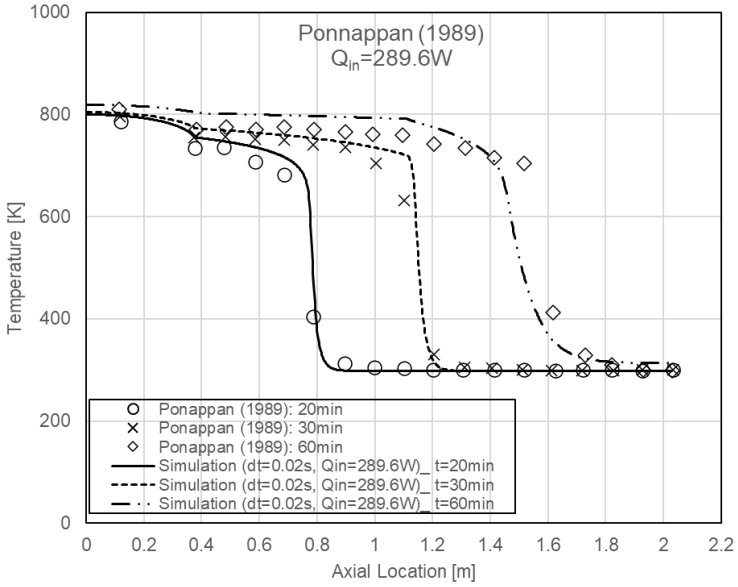

Figure 9. Predicted outer wall temperature compared against experiment of Ponnappan. [14]

3.2 Coupled Thermal-Structural Modeling, Code-to-Code Benchmark, and Preliminary Analysis of SPHERE Test

One of the crucial concerns with the heat-pipe cooled reactor is the large temperature gradient that occurred in the monolithic hex block during the heating/cooling stage, since larger temperature gradient will induce greater thermal stresses. To support the design and analysis on ongoing experimental work at the Single Primary Heat Extraction and Removal Emulator (SPHERE) facility at INL, two commercially available software packages (ABAQUS and STAR-CCM+) have been utilized in this report for a code-to-code comparison with both the temperature profiles and stress distributions for the single heat-pipe experiments. Finite Element Method (FEM) were used in both software simulations to estimate the temperatures and resultant thermal stresses to which the 7-hole core block for the SPHERE facility might experience during testing. Coupled thermal-structural analysis for the heat-pipe benchmark testing presented in this report can help to provide insights into the heat transfer mechanics of high-temperature heat-pipe experiments as well as the structural integrity of the experimental design aspects.

3.2.1 Modeling Method

As for the modeling strategy, computational analyses with ABAQUS and STAR-CCM+ have been completed with one-way coupling method. This means that the temperature distribution is solved with the heat transfer analysis at first, then using the temperature profile from the thermal analysis step as the boundary conditions (BCs) and start the stress analysis step using the same computational domain as the model setup. Only FEM solver is triggered for both heat transfer and stress analyses using ABAQUS and STAR-CCM+.

3.2.1.1 Model geometry, material properties, and initial & boundary conditions

Figure 10 shows the hex block geometry which was implemented in the coupled thermal-structural model; a single heat pipe is inserted in the central hole of the block, surrounded by six cartridge heaters (CHs) to simulate fuel rod heating.

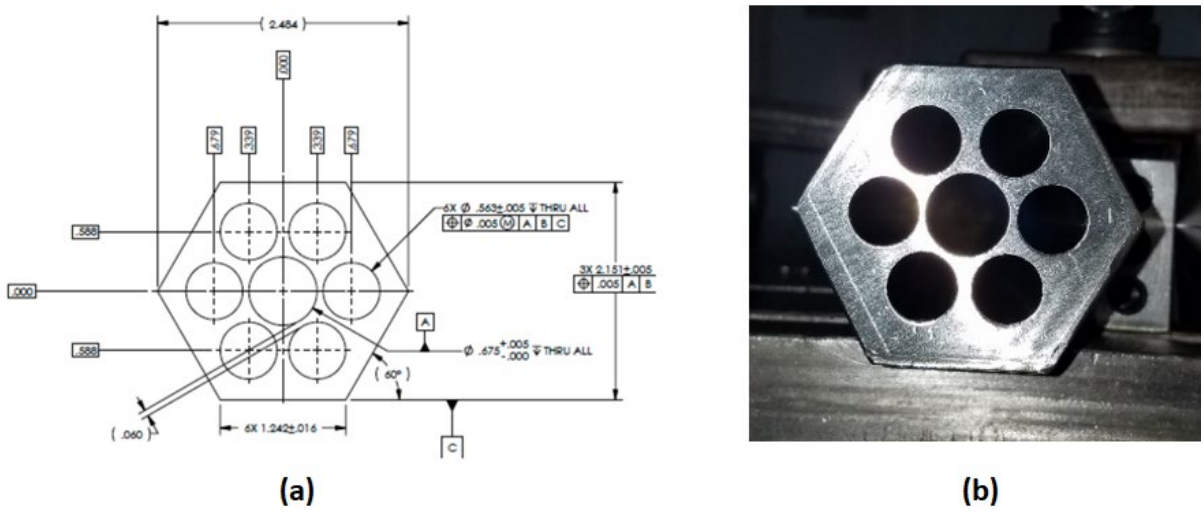

Figure 10. (a) Schematic for the hex block design adopted from [15] and (b) top-view of 7-hole hex block for the SPHERE facility.

Star-CCM+ 2020.m 15.06 was used to simulate the thermal stress behavior in the hex block. The program of version 15 provides capability of the calculation of stress field with FEM analysis. In the meantime, ABAQUS 2018.HF3 was also used to perform a code-to-code benchmark thermal and structural simulations on INL Falcon HPC system. The following assumptions (adopted from [16]) were made when modeling the single heat pipe test with both ABAQUS and STAR-CCM+:

- Dimensions were taken from previous reports [15, 16] for the case with a 152.4 mm (6") long hex block and CHs. Some important dimensions are summarized below:
  - HP: 15.88 mm (0.625") outer diameter (OD) × 14.45 mm (0.569") inner diameter (ID)
  - Center hex block hole diameter: 17.15 mm (0.675")
  - Diameter of 6 holes containing CHs: 14.30 mm (0.563")
  - CH OD: 12.70 mm (0.500").
- Quarter symmetry is assumed and ¼ of the hex block is modeled for the couple temperature-structural analysis (as shown in Figure 10.)
- The bottom of the model is set to be fixed (constrained not to move axially), while the plane symmetry is applied to the two side surfaces for the quarter hex block model (shown in (a) Schematic for the hex block design adopted from [15] and (b) top-view of 7-hole hex block for the SPHERE facility..)
- The inner surface of the HP was fixed at a constant temperature of 650°C (923.15K).
- The model is assumed to have an initial temperature of 20°C (293.15K).
- The total applied heat load was parametrically varied up to a maximum of 1,902 W (317 W per CH). The CHs were modelled as monolithic 304 stainless steel (SS304) with uniform volumetric heating. SS304 material properties are summarized in in Table 3.
- The hex block and the HP's sheath were modeled using the material properties of SS304 (details can be found in Table 3 and Table 4).
- The CH-to-hex block gaps and the hex block-to-HP gap were assumed to be filled by boron nitride (BN) paste. The BN paste was not included in the structural analyses currently, but this expansion phenomenon of BN will be investigated in the future study.
- Detailed material properties (for stainless steel and BN) are summarized in Table 3 and Table 4.
- The structural simulations only included elastic deformation, with no consideration of creep or plasticity in the model.
- Radial heat losses to the quartz tube and axial heat losses besides heat transferred to the HP were not included.

The mesh sensitivity studies with both the temperature and stress analyses have been performed to ensure the converged numerical solution with reasonable accuracy, which were not discussed in the report in details. Uniform hexahedral meshes was applied to the model geometry for both ABAQUS and STAR-CCM+. With the consideration of the simulation accuracy and computational cost, a uniform 1-mm mesh base size was used for all the coupled temperature-structural simulations with both software as shown in Figure 10.

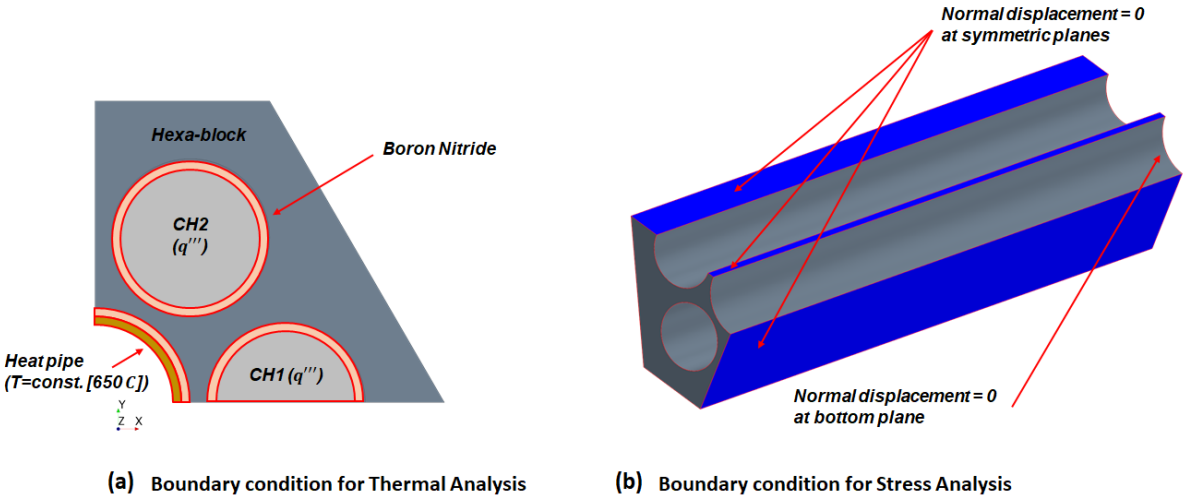

Figure 11. Boundary conditions for (a) thermal analysis and (b) stress analysis.

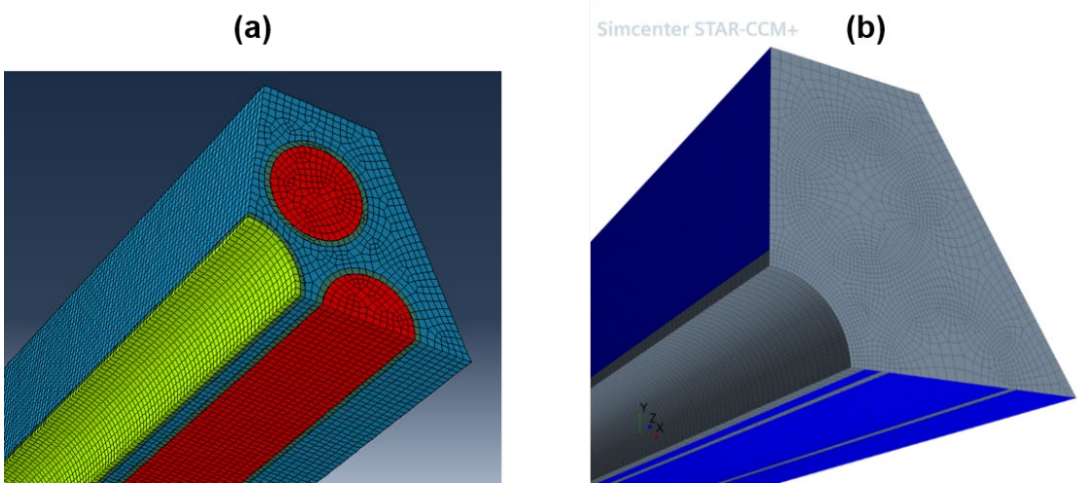

Figure 12. Mesh structure of test case (quarter block): (a) ABAQUS and (b) STAR-CCM+.

Table 3. Material properties used in the coupled thermal-structural analysis.

Material	Properties	Reference
SS304 (Hex block and CHs)	Density: 8055 kg/m^3 Specific heat: 480 J/kg-K Thermal conductivity: (see Table 4) Poisson's ratio: 0.31 Thermal expansion coefficient: (see Table 4) Young's modulus: (see Table 4)	[16]
Boron Nitride (Gap)	Density: 2000 kg/m^3 Specific heat: 840 J/kg-K Thermal conductivity: (see Table 4)	[16]

Table 4. Temperature-dependent mechanical properties of SS304 and BN. [16]

Property	Temperature (K)	Value
Thermal conductivity (W/m-K) for **SS304**	273.2	14.70
	300	15.20
	350	16.20
	400	17.00
	450	17.70
	500	18.40
	600	19.80
	700	21.20
	800	22.50
	900	23.90
	1000	25.30
	1100	26.70
	1200	28.10
	1300	29.50
	1400	30.90
	1500	32.30
	1600	33.70
	1665	34.70
Thermal Expansion Coefficient (1/K) for **SS304**	300	1.4290e-5
	407	1.4210e-5
	481	1.8720e-5
	579	1.9370e-5
	623	2.0060e-5
	765	1.9430e-5
	837	1.9260e-5
	908	1.9720e-5
	996	1.9940e-5
	1085	2.0680e-5
	1119	2.0270e-5
	1199	2.0890e-5
	1249	2.0890e-5
	1325	2.0920e-5
	1392	2.1360e-5
	1442	2.1300e-5
	1472	2.1410e-5
	1499	2.1390e-5
	1542	2.1450e-5
	1592	2.1750e-5
	1616	2.2160e-5

Property	Temperature (K)	Value
Young's Modulus (kg/m-s^2) for **SS304**	198	2.01E+11
	298	1.95E+11
	373	1.89E+11
	423	1.86E+11
	473	1.83E+11
	523	1.79E+11
	573	1.76E+11
	623	1.72E+11
	673	1.69E+11
	723	1.65E+11
	773	1.60E+11
	823	1.56E+11
	873	1.51E+11
	923	1.46E+11
	973	1.40E+11
Thermal conductivity (W/m-K) for **BN**	465.95	25.1
	663.15	22.5
	818.75	20.6
	970.95	18.7
	1095.45	17.4
	1244.35	15.7
	1372.05	14.6
	1520.95	13.1

3.2.2 Case Study Results and Discussion

Figure 13 and Figure 14 shows the temperature distributions as well as the Von Mises stresses contour plots in the hex block with both the top view and side view, using ABAQUS (upper) and STAR-CCM+ (bottom). These results were obtained with the total power input of 1,902 W (317W per CH), with a uniform mesh size of 1 mm. The maximum temperature locates on the outer surface of the hex block due to the adiabatic setting of the model, while the maximum Von Mises stress in the hex block happens at the inner surface of the heat-pipe hole. As expected, the outstanding thermal stress at this area is mainly caused by the temperature gradient between the heater and the heat pipe.

The Von Mises stress distribution contour shows that the maximum stress is located along the path between the centers of heat pipe and cartridge heaters as shown in Figure 15. The large temperature gradient at the shortest path results in the large stress. This result shows that the pitch between heat pipe and cartridge heater could be an important parameter for determining maximum thermal stress in the hex block. The pitch length would be calculated by the diameter of the heat pipe and cartridge, and thickness of the Boron nitride paste between hex block and components. Reducing the pitch would be helpful in decreasing temperature gradient. However, too small gap in the hex block between holes will increase the difficulty of the manufacturing of the holes in the hex block. Therefore, the parametric study for the pitch between holes considering manufacturing process should be considered in the future.

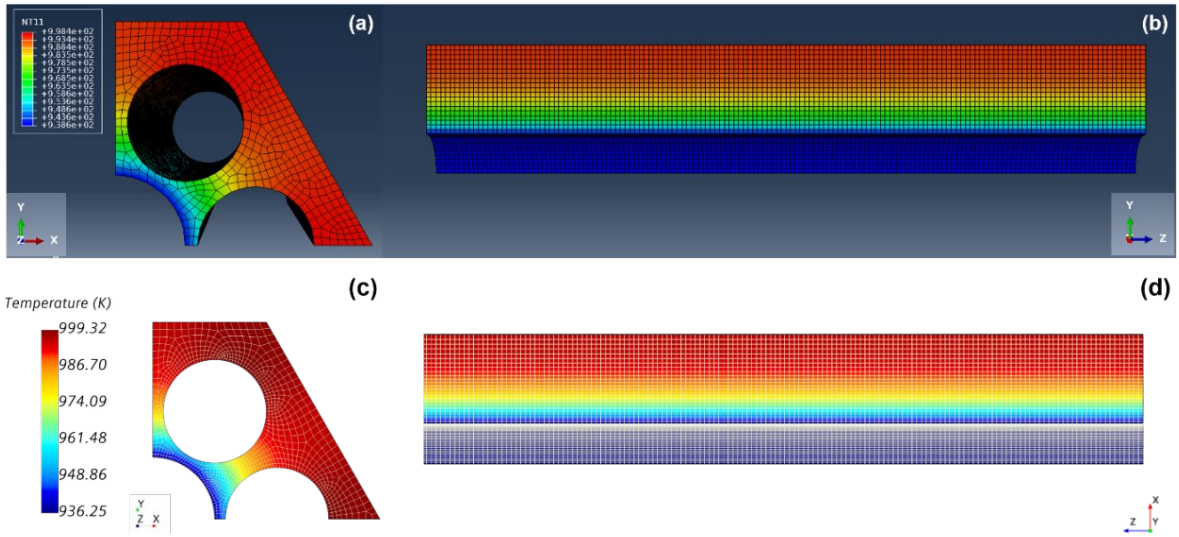

Figure 13. Temperature distribution with the heating power of 317W per CH at the top view (left) and side view (right) of the hex block (Upper: ABAQUS; Bottom: STAR-CCM+).

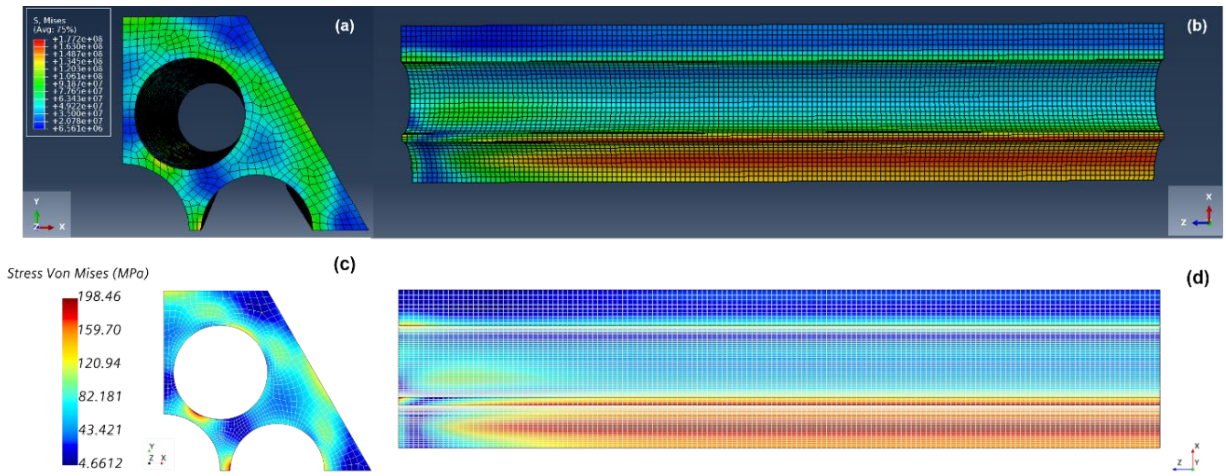

Figure 14. Von Mises stresses distribution with the heating power of 317W per CH at the top view (left) and side view (right) of the hex block (Upper: ABAQUS; Bottom: STAR-CCM+).

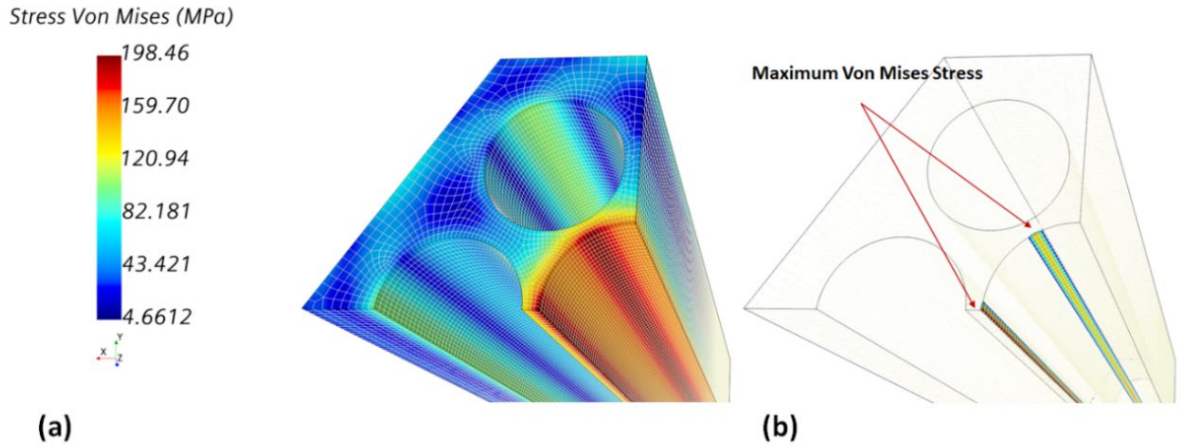

Figure 15. The location of the maximum von mises stress in the hex block.

The calculation result was verified by comparing the temperature field, thermal expansion coefficient field, and Young's modulus field as shown in Figure 16. Contours of thermal expansion coefficient and the Young's modulus at the bottom of the hex block. As thermal expansion coefficient and Young's modulus is dependent on the temperature; it is needed to confirm that proper value was applied with the temperature field. Figure 16 shows that the for the temperature range from 936.25 to 999.32 K, the TEC and the YM are properly calculated according to the material properties shown in Table 4.

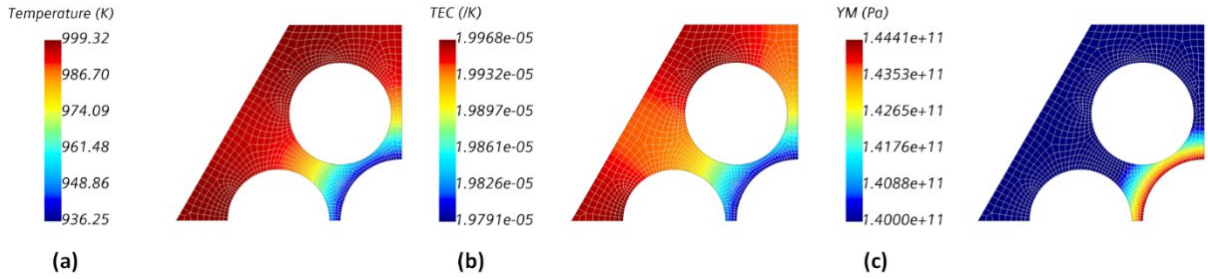

Figure 16. Contours of thermal expansion coefficient and the Young's modulus at the bottom of the hex block.

The parametric study for the coupled temperature-displacement analyses was performed in this report by changing the power of the cartridge heaters and observing the variation of the range of the temperature and the corresponding thermal stress. The heating power of 100% (317 W per CH), 50% (158.5 W per CH), and 25% (79.25 W per CH) were used while the other parameters and conditions remain the same. Table 5 summarizes the result from Abaqus and STAR-CCM+ for different power levels. Both temperatures and Von Mises stresses linearly increase according to the power levels in Abaqus and STAR-CCM+. The range of temperature of Abaqus and STAR-CCM+ are almost the same, while the range of the stress is higher in STAR-CCM+ in every cases.

The differences of the result are quantified by relative error calculated for STAR-CCM+'s results with the reference of Abaqus' and summarized in Table 5. The temperature calculations show good match between both software: the minimum and maximum temperature differences are all less than 0.3%. As the energy equation for the test section contains only conduction, the result is easy to be close for each other as expected. On the other hands, the minimum and maximum value of stress shows larger difference. For the minimum stresses, the results from STAR-CCM+ always has lower value. And for the maximum value, the result of STAR-CCM+ has larger value than that of ABAQUS. This indicates that the STAR-CCM+ will tend to predict higher stress than the ABAQUS.

Table 5. The temperature and stress range for the hex block with the different heating power.

Tool	Power Level	Temperature (°C)		Von Mises Stress (MPa)	
		Min.	Max.	Min.	Max.
Abaqus	25%	653.86	669.03	1.661	45.131
	50%	657.73	687.91	3.270	89.452
	100%	665.49	725.26	6.561	177.177
Star-CCM+	25%	653.49	668.96	1.146	48.608
	50%	656.99	687.78	2.265	96.638
	100%	664.02	725.01	4.488	190.83

Table 6. Percent difference of temperature and Von Mises stresses comparison between ABAQUS and STAR-CCM+.

Power Level	% difference in Temperature		% difference in Stresses	
	Min.	Max.	Min.	Max.
25%	-0.054	-0.010	-31.00	7.70
50%	-0.112	-0.018	-30.73	8.03
100%	-0.220	-0.034	-31.59	7.70

To investigate the difference of the stress values between Abaqus and STAR-CCM+ in detail, the stress components at the bottom plane (Z-) were plotted and compared. The Figure 17 shows the stress components in x, y, and z direction for both simulation tools. The distributions of the stress components are almost same. For stress component in x- and y- direction, the maximum values are observed at the gap between holes. For stress component in z-direction, the maximum stress exists at the peripheral of the center hole for the heat pipe. However, all the maximum stress of components are higher in Star-CCM+. As both simulations share same geometry, material properties, and same boundary conditions, the incomplete accordance between mesh structure could be a source of error, which should be considered in the future work.

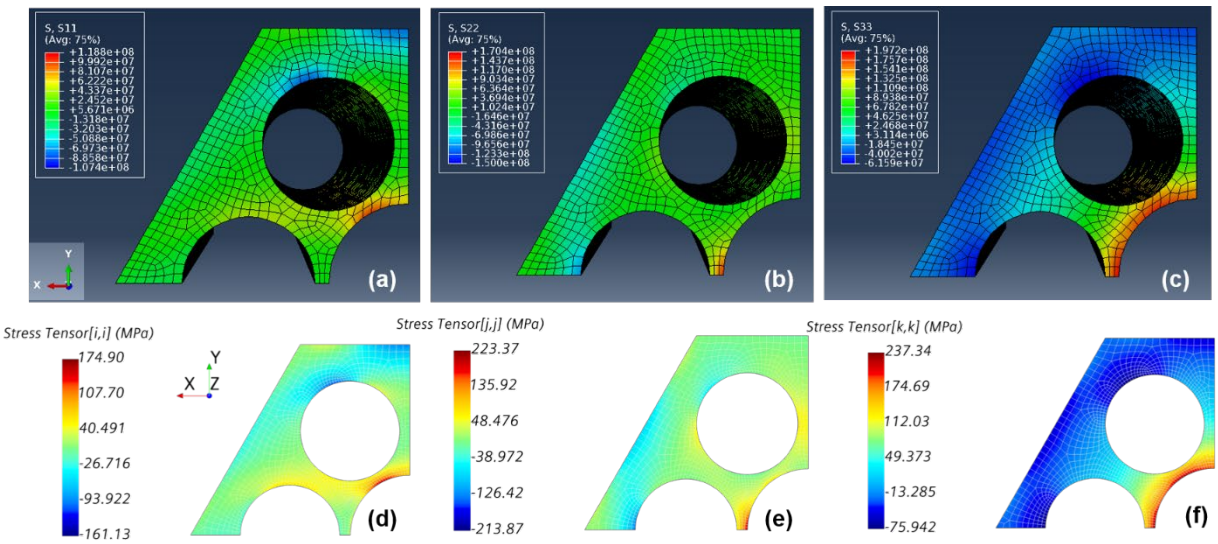

Figure 17. Contours of stress of the Von Mises stress in S11 (left), S22 (middle), S33 (right) normal directions (Upper: ABAQUS; Bottom: STAR-CCM+).

3.3 Summary and Path Forward

As of February 2021, the current status of modeling and simulation activities supported by the INL microreactor program can be summarized as follows:

1. Heat pipe modeling and analysis
   - Developed a theoretical basis for analyzing the entire startup process of liquid-metal heat pipe from frozen state based solely on transient heat conduction equations. Specifically, the effective

thermal conductivity of gaseous phase working fluid [i.e., Eqs. (22) and (23)] was derived based on the simplified mass and energy balance relations within a heat pipe.

- The conduction-based heat pipe analysis model was implemented into the commercial CFD software package, STAR-CCM+ for the heat pipe frozen startup simulation.
- The numerical simulation results were compared with the sodium heat pipe experimental data obtained by three different authors.
- The present conduction-based heat pipe analysis model was observed to predict the outer wall temperature of the sodium heat pipes, measured by the experiments, reasonably well.

2. Coupled thermal-stress modeling and analysis.
    - FEM-based coupled thermal-stress analysis model for the single heat pipe experiment in the SPHERE facility (7-hole core block test article) was created using the two commercial software packages, ABAQUS and STAR-CCM+.
    - The code-to-code benchmark study was performed to crosscheck the model setup and capability of each code, and to identify the potential concerns that may arise due to the excessive thermal stress or thermal coupling methods (e.g., BN) applied to the current experimental setup.
    - The profiles of temperature and Von Mises stress computed by ABAQUS and STAR-CCM+ were observed to agree well with each other, especially the locations where the maximum temperature and stresses happened in the geometry. While the temperature predictions were much closer (less than 0.3%), some deviations in stress results can still be noticed between these two software.

Based on the results and findings of our research so far, some future tasks are identified as follows:

1. Heat pipe modeling and analysis
    - Investigation into the performance of the present conduction-based heat pipe analysis model for higher power input cases.
    - Investigation on the extension of present model capability to heat pipe transient modes analysis.
2. Coupled thermal-stress modeling and analysis.
    - Further investigation into the potential cause of the difference in the stress analysis results between ABAQUS and STAR-CCM+ (e.g., mesh engine, temperature difference caused by material properties).
    - Future work: The constraints of the stress modeling on the test section will be changed to be consistent with the actual experimental constraints. The changes will include simulation on whole geometry with BN and heat pipe and the fixing of the hex block.
    - The parametric study for pitch between holes is needed to find optimized design value considering manufacturing tolerance of holes and temperature gradient at the gap.
    - The mesh structure is needed to be shared between simulations tool to reduce potential error from the mesh setups.

Current efforts will continue in the direction of validating the modeling and analysis capabilities established with the data that will be generated from the single heat pipe experiments (7-hole core block test) and guiding the experimental test plans. The initial validation effort will particularly focus on the startup phase of the heat pipe-cooled system with the sodium heat pipe. Furthermore, the thermal stress behavior could be better characterized and understood with the experimental data from the strain gauges that will be installed in the future.

4. SOCKEYE GAP ANALYSIS AND V&V PLAN

Software verification and validation (V&V) hold an important role in the safety analysis for nuclear facilities, as the codes and models utilized in calculations demonstrating the safety basis as part of DOE authorization must demonstrate an acceptable pedigree. To that end, a strategy to support verification and validation of the Sockeye system-level safety analysis software applied to heat pipe design and applications has been developed.

The overall goal of the Sockeye V&V effort is to demonstrate the suitability of the code for evaluation of safety performance and characterization of safety margins for heat pipes. The V&V methodology will be used to demonstrate the adequacy of the Sockeye component and physical models for the corresponding heat pipe design elements [17].

4.1 Sockeye Verification and Validation Approach

The V&V methodology developed has been derived in part from the evaluation model development and assessment process (EMDAP) in Regulatory Guide 1.203 [18], “Transient and Accident Analysis Method”. Note that typically EMDAP is applied to the software and its associated inputs used to model a specific plant configuration and transient. Thus, the methodology has been adopted and modified to be suitable for V&V for a range of heat pipe conditions. It is also worth noting that EMDAP requires usage of an appropriate quality assurance (QA) standard and development of supporting documentation for development and assessment of the evaluation model (EM). Because Sockeye is actively in development, this requirement may not be practical at all times. Balance between the code capabilities, heat pipe design constraints and QA need to be determined prior to establishing a path forward. The extent of the EMDAP methodology has been adapted for practical and flexibility considerations.

For the objectives of this work, unless otherwise noted the following definitions will be used:

- Verification: the act of reviewing, inspecting, testing, checking, auditing, or otherwise determining and documenting whether items, processes, services, or documents conform to specified, discrete requirements.
- Validation: confirmation, through the provision of objective evidence, that the requirements for a specific intended use or application have been fulfilled.

That is, verification is considered to be a series of reviews to determine compliance with de- fined incremental requirements (e.g., constituent-level determination of acceptance). Validation is considered to be evaluations against experimental data, theoretical solutions, code-to-code comparisons, standardized problems with known solutions, and published data and correlations. Verification is typically considered to be a stepwise comparison of incremental results to requirements of an individual step, and validation to be an overall comparison of the final result to over-arching requirements.

4.2 The Sockeye Code

Sockeye is an application that models heat pipe performance, based on the MOOSE framework. Its primary focus is on liquid-metal heat pipes with annular screen or porous wick structures, with the intended application being the simulation of heat pipes in microreactors.

Sockeye is being developed as a transient heat pipe modeling and simulation tool, and simulation capabilities for various microreactor heat pipe designs. The Sockeye heat pipe code specific characteristics are as follows:

- Utilizes an object-oriented application framework (MOOSE [19]).
- Incorporates advances in the physical and empirical models for heat pipe analysis leveraging models developed over several decades and new multiphase models.
- Provides multi-scale, multi-physics modeling capabilities by integrating with other higher-fidelity advanced simulation tools.

4.3 Sockeye Modeling Requirements

This section focuses on the identification of critical characteristics and acceptance criteria as they relate to software performance and modeling capabilities.

To that end, a set of cross-cutting phenomena relevant to heat pipe characteristics and operational conditions has been identified for the purpose of evaluating Sockeye implementation and testing with regard to the ability to model a wide-range of phenomena per the qualification and dedication requirements.

4.3.1 Operation Conditions

Code requirements need to be considered with respect to the operating conditions modeled. Overlap can occur between these operating conditions and requirements will be similar. Sockeye shall be capable of modeling the following operating conditions:

- Start-Up
- Steady-State Operation
- Transient Operation
- Shutdown

These operating conditions are applicable for both normal operating and accident conditions.

4.3.2 Normal Operating Conditions

Sockeye shall have the following modeling capabilities when simulating heat pipe nor- mal operating conditions.

- Sockeye shall calculate the heat pipe operational limits.
- Sockeye shall compute heat pipe thermal-hydraulic conditions for normal operation.
- Sockeye shall be able to simulate a standalone heat pipe.
- The code shall be capable to simulate a single or multiple heat pipes coupled with a core or a heat exchanger.
- Sockeye shall be capable to model three phases (solid, liquid and gas) in heat pipes to simulate the identified operating conditions.
- Sockeye shall be capable of simulating the following boundary conditions:
  - Specified temperature function
  - Specified heat flux function
  - Temperature-dependent heat flux
- Sockeye shall be able to incorporate the effects of the following properties:
  - The thermal resistance of the working fluid.
  - The thermal resistance of the wick layer.
  - The thermal resistance of the heat pipe cladding.
- The code shall provide a functionality to calibrate the capillary pressure predictions.
- Sockeye shall be able to model and characterize the wet point (equal liquid and gas pressure) outside of the evaporator region.
- Sockeye shall be capable of simulating the partial contact of the heat pipe to the evaporator.

- The code shall compute the thermo-physical properties of the heat pipe wall:
  - Thermal Conductivity
  - Density
  - Heat Capacity
- Sockeye shall simulate wall boiling to capture the impact of high initial heat fluxes at the condenser for the different operating conditions.
- Sockeye shall be capable to model non-condensable gases in heat pipe for the different operating conditions.

4.3.3 Accident Conditions

In addition to the normal operating condition modeling capabilities, Sockeye shall model accident conditions where margins to heat pipe failure can be determined.

- Sockeye shall model individual heat pipe failure. As such, the following conditions shall be fulfilled:
  - The code shall be capable to check the heat pipe limits.
  - The code shall change heat flux conditions when failure occurs.
- Sockeye shall be capable of simulating various transient conditions:
  - Reduced heat removal in heat exchanger.
  - Core power excursion.
- Sockeye shall allow user-specified wall and interfacial drag models.
- Sockeye shall allow user-specified constant user-specified friction factor with a correlation dependent on Reynolds number (and possibly wick permeability).
- Sockeye shall be capable of simulating the following boundary conditions:
  - Specified temperature function
  - Specified heat flux function
  - Temperature-dependent heat flux

4.4 Sockeye Validation Gap Analysis

A listing of validation gaps has been developed in the table below as they relate to software qualification. These gaps have been derived from the summary requirements identified in Section 4.3. Additional discussion of these gaps is provided below.

Table 7. Sockeye Validation Gap Prioritization.

Gap	Comment
SET/IET Validation	Code qualification reports describing the qualification of the EM against separate effects test data, integral system effects tests and heat pipe data are needed.
Valid Numerical Model Bounds	Code qualification which details the range of applicability of the important basic models and correlations based on separate effect tests and sensitivity analyses is needed. Results and associated uncertainties applicable to such models need to be incorporated into the software qualification record.

Gap	Comment
Valid Input Bounds	Code Manual and model qualification documentation is needed to detail the acceptable input value bounds. These bounds can be based on model uncertainty quantification and sensitivity analyses.
Default/Suggested Inputs	Code manual and model qualification documentation is needed to detail default or suggested input values where the latter is not available to the code user. These values can be based on model uncertainty quantification and sensitivity analyses.

As indicated in the table above, demonstration of the Sockeye numerical model validity and characterization of model applicability range depends upon the determination of the experimental and numerical uncertainties associated with the SET/IET benchmark cases. Simulation uncertainties are generally determined based on geometric and modeling parameters, material properties, and modeling assumptions. In order to assess the effects of the uncertainties and determine the safety margins for a specific heat pipe design, uncertainty quantification (UQ) and sensitivity analysis are required. Quantifying these experimental uncertainties is paramount to determining the Sockeye model inherent numerical error.

Sensitivity analyses, on the other hand, are important to explore the sources of variability in computational results. For code validation, the experimental uncertainty, which is composed of measurement, material, and geometry uncertainties, needs to be known. Sockeye numerical model and correlation uncertainty is likely to be best characterized for smaller, focused experiments such as SETs.

Experimental uncertainties shall be provided by the owners of the experiment data. Sockeye model overall uncertainty is likely to be best quantified through qualification analyses of larger experiments, such as IETs, where interactions between the various components in the system are studied. The code validation process aims at identifying the constituents of the model uncertainty such as experimental and numerical correlation uncertainties on a larger scale to be able to characterize Sockeye model overall uncertainty.

4.5 Validation Tests

Collection of experimental data for high-temperature heat pipes is challenging. Instrumentation must be able to withstand these high temperatures, and installation of instrumentation on the inside of a heat pipe potentially affects the flow field.

Most experimental data for high-temperature heat pipes is limited to externally mounted thermocouples; however, some experimentalists have measured internal data, such as vapor temperature. Section 4.5.2 identifies past experiments that are potential validation cases.

4.5.1 Material Properties

Sodium properties are well documented within the scope of pool-type Sodium fast reactors [21] and these properties tend to be focused for fast reactor applications. Reference [21] documents the critical constants of sodium. Additionally, it incorporates enthalpy data and documents Sodium properties covering subcooled and superheated as well as saturated sodium properties. Additional review is needed to ensure that the ranges of temperatures and pressures documented in the literature cover the ranges needed for heat pipe applications.

4.5.2 Experimental Facilities

The following past experiments have been identified as potential validation cases:

- SAFE-30 heat pipe. In this experiment, a sodium/stainless steel heat pipe was attached to 4 cartridge heaters in a vacuum chamber. Thermocouples were mounted on 3 locations on the "fuel" tubes containing the cartridge heaters and 5 axial locations on the surface of the heat pipe cladding. A 5-hour power ramp (up to 2600 W electrical power) and cooldown was performed from the frozen state. The thermocouple data and measured powers have been provided to the Sockeye team.
- SAFE-100 thermal heatpipe. SAFE-100 is a 100-kilowatt thermal heat pipe concept which passively extracts the heat from fission via liquid metal heat pipes to heat exchangers. In the SAFE-100 heat exchanger, the size of the coolant annulus also varies with radial position across the core to maintain adequate cooling radially across the bank of heat pipes emerging from the reactor core. For testing purposes, only the central flow channel was constructed.
- SAFE-100a fission reactor. The SAFE-100a experiment is a thermal simulation of an in- space nuclear reactor core. The heat created by the nuclear fission process is simulated by electric heaters placed in the core fuel pins where the uranium would normally be. The heat from the core is transported out of the core via sodium-filled heat pipes that extend out of the core on one side. The heat pipes pass through a heat exchanger (HX) that extracts heat from the pipes and transfers it into a helium argon gas mixture. This heated gas would then be used to drive an electric generator.
- High-temperature heat pipes with multiple heat sources. In these experiments, a sodium/stainless steel heat pipe designed to operate in a vapor temperature range of 500- 800 ˚C was fitted with 4 heaters (in different axial sections) and subjected to different combinations of powers to each. Additional dimensions to the experiments included the ambient condition (air vs. vacuum), the working fluid fill level (two cases were tested), and inclination of the heat pipe with respect to gravity (a few angles near the horizontal were tested). Data was collected from 12 wall thermocouples, 6 vapor space thermocouples, and calorimeters in the evaporator, transport, and condenser sections. Regimes studied included startup, continuum transient, and steady state.
- The Kilowatt Reactor Using Stirling TechnologY (KRUSTY) test program [25]. KRUSTY was a prototypic nuclear-powered test of a 5-kW(thermal) Kilopower space reactor. 2 Kilopower reactor concepts utilize heat pipes to transfer fission energy from a solid block of fuel and are intended for simple, low-power [1- to 10 -kW(electric)] space and surface power systems.
- Single primary heat extraction and removal emulator (SPHERE) facility and capability is designed and being developed to support non-nuclear thermal and integrated systems testing, for better understanding of thermal performance of the heat pipe under a wide range of heating values and operating temperatures, further enhancing understanding of heat pipe startup and transient operation. As more progress is made the experimental group will be performing calorimetric measurements with water-cooled gas-gap calorimeter, determining heat-pipe operational limits, and testing under both air and inert gas conditions. The capability of the facility allows for detailed testing, enabling understanding startup and transient behavior as these are expected to be utilized in remote locations and will need to load follow.
- Preliminary Microreactor AGile Non-nuclear Experimental Testbed (MAGNET) is one component in the Dynamic Energy Transport and Integration Laboratory (DETAIL). It is a facility that will allow demonstration of a variety of integrated energy system (IES) configurations. MAGNET will first analyze a heat-pipe microreactor design. For heat pipe microreactor development, understanding the potential effects of a cascading failure caused by the failure of one heat pipe in a core is vital along with understanding the corresponding thermal stresses and heat transfer, respectively. MAGNET provides a test platform to perform such testing along with furthering the understanding of interface coupling challenges with Power Conversion Unit and other collocated systems.

In addition to existing heat pipe data, two NEUP experimental studies are scheduled to pro- duce data that will support Sockeye validation:

- NEUP Project 20-19735: Experiments for Modeling and Validation of Liquid-Metal Heat Pipe Simulation Tools for Micro-Reactors. Normal operation, as well as the transient behavior of frozen startup, shutdown, and restart will be studied. The temperature distribution in the core, wick, annular gap, and external wall surface will be measured by a fiber- optic distributed temperature sensor and thermocouples. Pressure will be measured using pressure-transfer-liquid techniques. Phase distribution will be measured using X-ray systems. These experiments are expected to yield data in 2022.
- NEUP Project 19-17416: Experiments and computations to address the safety case of heat pipe failures in Special Purpose Reactors. Startup, shutdown, and normal operation will be studied at different inclinations. Thermocouples and optic fibers will be installed in all axial regions, on the outside of the heat pipe. High-resolution X-ray imaging will be used to measure void fraction. Thermomechanical stresses on the core structure after multiple pipe failures will be measured.

4.6 Sockeye Verification and Validation Plan

Table 8. Sockeye Validation Plan.

	SAFE-30 [22]	SAFE-100 [23]	SAFE-100a [24]	KRUSTY [25]	SPHERE [28]	MAGNET [29]	SPR [27]	TAMU [26]	Faghri [11][12]	CFD [20]
Material Properties										
Working Fluid Properties			X							
Wick Characteristics								X		
Wall Properties		X	X							X
Physical Phenomena										
Capillary Pressure										
Liquid Pressure Drop		X						X		
Vapor Pressure Drop								X	X	
Wall Convective Heat Transfer	X	X	X	X						
Wall Conduction Heat Transfer	X	X	X	X						
Interfacial Mass Transfer										
Interfacial Heat Transfer										
Experimental Data										
Vapor Temperature Distribution			X					X	X	
Liquid Temperature Distribution		X	X	X	X					
Phase Distribution							X	X		
Friction Factors								X		X

	SAFE-30 [22]	SAFE-100 [23]	SAFE-100a [24]	KRUSTY [25]	SPHERE [28]	MAGNET [29]	SPR [27]	TAMU [26]	Faghri [11][12]	CFD [20]
Operation Limits										
Capillary Limit									X	
Boiling Limit										
Sonic Limit	X	X		X					X	
Entrainment Limit									X	
Viscous Limit		X		X						
Operational Modes										
Normal Operation							X	X	X	
Frozen Startup	X			X	X		X	X	X	
Frozen Startup Limit								X		
Shutdown	X				X			X		
Re-Start					X			X		
Pipe Failure				X		X		X		

4.7 Sockeye Needs

The use of existing heat pipe experimental data is challenging for use of software validation. Instrumentation precision, accuracy of the measurements and experimental processes need to be well documented for a rigorous validation. Additionally, instrumentation operational limitations and precision need to be characterized.

Ideally, the measurements obtained are of high spatial and temporal resolution to be able to capture smaller scale phenomena.

Because Sockeye is not able to model complex wick geometries, limitations exist in the modeling of experimental facilities where internal heat pipe temperatures are obtained via a central thermowell. An instrumentation set that can measure interior heat pipe conditions while not being invasive as to perturb the proper function of the heat pipe is ideal.

Additionally, information on the experimental environment is crucial for accurate modeling. Information on the nature and properties of the heat pipe surrounding environment need to be documented as well as the temperature of the surroundings (at initial conditions and during the experiment). Material composition, size and location of neighboring components will help quantify the heat transfer from the environment to the heat pipe cladding. As such, the information is needed to properly define heat pipe boundary conditions.

The ideal datasets for Sockeye validation should include:

- Characterization of wick parameters (porosity, permeability, capillary pressure). These are Sockeye inputs, as they cannot be accurately predicted. Therefore, proper measurements of these parameters are needed for accurate validation, specifically for modeling capillary pressure and limit.
- Identity and mass of non-condensable gases (NCGs) inside heat pipe

5. SUMMARY AND FUTURE PLAN

This report summarizes the modeling and simulation activities under DOE microreactor program to support ongoing single heat pipe experiments with 7-hole core block at the SPHERE facility. The primary objective of these activities is to obtain preliminary insights into the current single heat pipe-cooled experimental facility, and based on that, support and guide the experimental efforts and test plans with the aim of producing high-quality experimental data.

Considering the current major interests of the single heat pipe experiment, i.e., (i) the startup behavior of liquid-metal heat pipe and (ii) the thermal stress of structural materials under high temperature operating conditions, the modeling and simulation efforts are being made in two respects:

1. Development of a simplified conduction-based heat pipe analysis method for analyzing the liquid metal (sodium) heat pipe startup from a frozen state.
2. A coupled thermal-structural modeling and analysis for SPHERE experiment (with 7-hole core block) and code-to-code benchmark.

As of February 2021, the theoretical development of the conduction-based heat pipe startup analysis model and the preliminary model performance tests using commercial CFD software have been completed. Also, the FEM-based coupled thermal-stress analysis model for the ongoing single heat pipe experiment has been created using the two commercial software packages (ABAQUS and STAR-CCM+), and the code-to-code benchmark study has been performed. The analysis results have led us to identify the limitations of the current models and future tasks for model improvement and validation.

Efforts will continue to use and further develop the modeling and analysis capabilities that have been built so far, to support ongoing single heat pipe experimental activities at the SPHERE facility such as measurement planning, data analysis, and potential design improvement study. Potential cooperation with Oak Ridge National Laboratory (ORNL) will equip us with some cutting-edge sensor technologies like embedded metallized optical fibers [30-32] for high temperature strain measurements in SPHERE and MAGNET facilities. In addition, continuing collaboration with the NEAMS program using the MOOSE framework is considered important so that the experimental data from SPHERE and MAGNET facilities can satisfy the validation needs of Sockeye, a system-level heat pipe modeling software being developed with the support of DOE.

6. REFERENCES

1. Cao, Y. and A. Faghri, "A numerical analysis of high-temperature heat pipe startup from the frozen state," *ASME Journal of Heat Transfer*, vol. 115, no. 1, pp. 247-254. 1993. https://doi.org/10.1115/1.2910657

2. Yuan, Y., et al., "Study on startup characteristics of heat pipe cooled and AMTEC conversion space reactor system," *Progress in Nuclear Energy*, vol. 86, pp. 18-30. 2016. https://doi.org/10.1016/j.pnucene.2015.10.002

3. Faghri, A., *Heat pipe science and technology*. 1995: Global Digital Press.

4. Ma, M., et al., "A pure-conduction transient model for heat pipes via derivation of a pseudo wick thermal conductivity," *International Journal of Heat and Mass Transfer*, vol. 149, p. 119122. 2020. https://doi.org/10.1016/j.ijheatmasstransfer.2019.119122

5. Tournier, J.M. and M.S. El-Genk, "A vapor flow model for analysis of liquid-metal heat pipe startup from a frozen state,. *International Journal of Heat and Mass Transfer*, vol. 39, no. 18, pp. 3767-3780, 1996.

6. Zuo, Z. J., and Amir Faghri. "A network thermodynamic analysis of the heat pipe." International Journal of Heat and Mass Transfer 41.11 (1998): 1473-1484.

7. Sobolev, V., "Database of thermophysical properties of liquid metal coolants for GEN-IV," SCK CEN No. BLG-1069, 2011.

8. Hsiao, J., "An efficient algorithm for finite-difference analyses of heat transfer with melting and solidification," *Numerical Heat Transfer*, vol. 8, no. 6, pp. 653-666, 1984. https://doi.org/10.1080/01495728508961877

9. Wang, C., et al., "Study on the characteristics of the sodium heat pipe in passive residual heat removal system of molten salt reactor," *Nuclear Engineering and Design*, vol. 265, pp. 691-700, 2013. https://doi.org/10.1016/j.nucengdes.2013.09.023

10. Chi, S., "Heat pipe theory and practice," Washington, D.C., Hemisphere Publishing Corp.; New York, McGraw-Hill Book Co., 1976.

11. Faghri, A., M. Buchko, and Y. Cao, "A study of high-temperature heat pipes with multiple heat sources and sinks: Part II—Analysis of continuum transient and steady-state experimental data with numerical predictions," *Journal of Heat Transfer*, vol. 113, no. 4, pp. 1010-1016, 1991. https://doi.org/10.1115/1.2911194

12. Faghri, A., M. Buchko, and Y. Cao, "A study of high-temperature heat pipes with multiple heat sources and sinks: Part I—Experimental methodology and frozen startup profiles," *Journal of Heat Transfer*, vol. 113, no. 4, pp. 1003-1009. 1991. https://doi.org/10.1115/1.2911193

13. Buchko, M., "Experimental Investigation of Low and High Temperature Heat Pipes With Multiple Heat Sources and Sinks," Master's Thesis, Wright State University, Dayton, OH, 1990.

14. Ponnappan, R., "Studies on the startup transients and performance of a gas loaded sodium heat pipe," 1989, Universal Energy Systems, Inc., Dayton, Ohio.

15. Trellue, H.R., et al., "Microreactor Agile Nonnuclear Experimental Testbed Test Plan," 2020, Los Alamos National Laboratory (LANL): Los Alamos, NM. https://doi.org/10.2172/1595649

16. Petrie, C.M. and N.D.B. Ezell, "Demonstrate embedding of sensors in a relevant microreactor component," 2020, Oak Ridge National Laboratory (ORNL), Oak Ridge, TN. https://doi.org/10.2172/1720216

17. Hansel, J.E, Berry, R.A., Andrš, D. and Martineau, R.C., "Sockeye Theory Manual," INL Report INL/EXT-19-54395, Idaho National Laboratory, 2020. https://doi.org/10.2172/1697979

18. Transient and Accident Analysis Methods, Tech. Rep. Regulatory Guide 1.203, U.S. Nuclear Regulatory Commission, 2005.

19. Permann, C.J., Gaston, D.R., Andrš, D., Carlsen, R.W., Kong, F., Lindsay, A.D., Miller, J.M., Peterson, J.W., Slaughter, A.E., Stogner, R. H. and Martineau, R. C., "MOOSE: Enabling Massively Parallel Multiphysics Simulation," *SoftwareX*, vol. 11, p. 100-130, 2020. https://doi.org/10.1016/j.softx.2020.100430

20. Shaver, D.R., and Tentner, A., "Calculation of Friction Factors in Heat Pipes using CFD in Support of the Sockeye Code," ANL Report ANL/NSE-20/47, Argonne National Laboratory, 2020. https://doi.org/10.2172/1734864

21. Fink, J. K., and Lebowitz, L., "Thermophysical Properties of Sodium," Technical Report ANL-CEN-RSD-79-1, Argonne National Laboratory, 1979.

22. Reid, R. S., Sena, J. T., and Martinez, A. L., "Sodium Heat Pipe Module Test for the SAFE-30 Reactor Prototype," AIP Conference Proceedings, vol. 552, no. 1, pp. 869–874, 2001. https://doi.org/10.1063/1.1358021

23. Martin, J., and Salvail, P., "Sodium Heat Pipe Module Processing fort he SAFE-100 Reactor Concept, AIP Conference Proceedings," vol. 699, no. 1, pp. 148–155, 2004. https://doi.org/10.1063/1.1649569

24. Steeve, B., "Safe Affordable Fission Engine- (SAFE-)100a Heat Exchanger Thermal and Structural Analysis," Technical Report NASA/TM—2005–213609, NASA, 2005. https://ntrs.nasa.gov/citations/20050166900

25. Poston, D. I., Gibson, M. A., Sanchez, R. G., and McClure, P. R., "Results of the KRUSTY Nuclear System Test," *Nuclear Technology*, vol. 206, no. sup1, pp. S89–S117, 2020. https://doi.org/10.1080/00295450.2020.1730673

26. Lee, S., "NEUP Project 20-19735: Experiments for Modeling and Validation of Liquid-Metal Heat Pipe Simulation Tools for Micro-Reactors," Technical Abstract, Texas A&M, 2020.

27. Petrov, V., "NEUP Project19-17416: Experiments and Computations to Address the Safety Case of Heat Pipe Failures in Special Purpose Reactors," Technical Abstract, University of Michigan, 2019.

28. Sabharwall, P., Hartvigsen, J., Morton, T., Sellers, Z., Yoo, J.S., "SPHERE Assembly and Operation Demonstration," INL/EXT-20-60782, Revision 0, Idaho National Laboratory, 2020.

29. Morton, T.J., O'Brien, J.E., Hartvigsen, J.L., "Functional and Operating Requirements for the Microreactor Agile Non- Nuclear Experimental Test Bed (MAGNET)," INL/EXT-20-58104, Revision 0, Idaho National Laboratory, 2020.

30. Petrie, Christian M., and Nora Dianne Bull Ezell. Demonstrate embedding of sensors in a relevant microreactor component. No. ORNL/SPR-2020/1742. Oak Ridge National Lab.(ORNL), Oak Ridge, TN (United States), 2020. https://doi.org/10.2172/1720216

31. Petrie, Christian M., et al. "High-temperature strain monitoring of stainless steel using fiber optics embedded in ultrasonically consolidated nickel layers∗." Smart Materials and Structures 28.8 (2019): 085041. https://doi.org/10.1088/1361-665X/ab2a27

32. Petrie, Christian M., et al. "Embedded metallized optical fibers for high temperature applications." Smart Materials and Structures 28.5 (2019): 055012. https://doi.org/10.1088/1361-665X/ab0b4e